



Numerical classification of termite-mediated soils along toposequences and rangeland use influenced soil properties in southeast Ethiopia

Abinet Bekele^{a,*}, Sheleme Beyene^b, Fantaw Yimer^c, Alemayehu Kiflu^b

^a Department of Plant Science, College of Agriculture, Bule Hora University, P. O. Box 144, Bule Hora, Ethiopia

^b School of Plant and Horticultural Science, College of Agriculture, Hawassa University, P. O. Box 05, Hawassa, Ethiopia

^c Wondo Genet College of Forestry & Natural Resources/ Hawassa University, P. O. Box 128, Shashemane, Ethiopia

ARTICLE INFO

Keywords:

Clustering
Cultivated land
Enclosure
Open-grazing land
Pedogenic processes

ABSTRACT

Despite termite-induced soil mixing, summarizing termite-affected soil horizons is difficult, while the lack of accurate information on the pedogenic processes featured by termite bioturbation, topography, and land use limits an effort to address land degradation. A study was therefore carried out to quantitatively classify the soils and describe them based on rangeland uses. Based on cluster analysis, five representative soil profiles were studied at different topographical positions. Soil samples were collected from mounds and adjacent soils under enclosure, cultivated, and open-grazing land at the summit and foot slope positions. Agglomerative clustering showed low Ca^{2+} , CEC, pH, and Mg^{2+} that described cambic horizons formed Cambisols at the summit and back slope. Eluviation-illuviation processes formed Luvisols on the toe slope and foot slope, whereas clay and high CEC described argic horizons. High Ca^{2+} , CEC, pH, and Mg^{2+} described calcic horizons that formed Calcisols on the bottom slope. Divisive clustering showed that soil properties varied slightly between Cambisols and Luvisols at different topographies. However, the Luvisols on the toe slope were differentiated from the soil on the foot slope by predominant pedogenetic clay formation and a distinctly increased CEC. Calcisols are placed in other clusters due to their distinct properties. Agglomerative clustering reflected pedogenic processes and differentiated diagnostic horizons, while divisive clustering matched WRB classification. The results of this study also showed that termite-mediated soil properties were dictated by rangeland use, and pedogenesis was more noticeable on open-grazing land than on enclosure or cultivated land.

1. Introduction

Termites are an important agent of pedogenesis, affecting soil ecosystem functioning in arid and semi-arid regions [1–4]. As key bioturbators, termites affect soils by loosening, selecting, translocating, and mixing various soil particles to maintain the functional properties of their mounds [5]. Termites also influence the amount of soil mixed and the rate at which materials are deposited on the surface, the amount of accumulated soil materials, and their redistribution over the surface as outwash pediments [6,7].

* Corresponding author.

E-mail addresses: abibekelema@gmail.com, aabinet.bekele@bhu.edu.et (A. Bekele), shelemeb@gmail.com (S. Beyene), fantawyimer2003@yahoo.com, fantawyimer2003@gmail.com, fantaw.y@hu.edu.et (F. Yimer), alemanchy@gmail.com (A. Kiflu).

<https://doi.org/10.1016/j.heliyon.2023.e23726>

Received 4 May 2023; Received in revised form 11 December 2023; Accepted 12 December 2023

Available online 16 December 2023

2405-8440/© 2023 The Authors. Published by Elsevier Ltd. This is an open access article under the CC BY-NC-ND license (<http://creativecommons.org/licenses/by-nc-nd/4.0/>).

Vertical and horizontal movements of ingested and transported material within the soil mediated by burrowing invertebrates are less influential in modifying pedogenesis in the short term [8]. However, termites modify soil and mound properties depending on several environmental factors [5,9]. For instance, topography, which affects soil formation, determines the structural formation of termite mounds [10]. According to Muvengwi and Wilkowski [11], termite-driven heterogeneity and topography play a major role in the variation of soil properties. As an anthropogenic activity, the type of land use practices in a given area is important in controlling soil heterogeneity at the landscape level [12,13]. Landscape heterogeneity strongly influences termite activities. According to Leclare et al. [2], termite activities are promoted by diverse habitat patches while being reduced by a fragmented landscape. For *Odontotermes* and *Macrotermes* species, Kaiser et al. [14] estimated about 216 and 32 t of soil material per ha per month on rehabilitative and barren land, respectively. This is because land use change results in termite species and diversity alterations [15]. Accordingly, when termites are involved in surface deposition and subsequent erosion from the mounds [16] with further downslope displacement, the soil ecosystem will be complex at the landscape scale, and termite pedoturbation will become more apparent.

A better mechanism to obtain sufficient soil information in complex landscapes is through proxy environmental characteristics that reveal soil properties, topographical positions, and vegetation compositions [17,18]. Frequently, soil information is obtained through the most widely used soil taxonomy, the USDA soil taxonomy (ST) [19] and the World Reference Base (WRB) [20]. In these classification systems, high variability has been reported for many soil orders [21]. For example, Esfandiarpour-Boroujenia et al. [22] reported a poor correlation between these two systems in arid and semi-arid Iranian soils. According to Balla et al. [23], qualifiers applied to certain ST soil groups are limited in WRB. Although these classification systems take into account the soil-forming processes in diagnostic characteristics, they do not accentuate the role of soil-forming processes in soil classification [20,24].

Unlike ST and WRB classification systems, numerical soil taxonomy has been advocated for a century, and the future soil classification system is likely geared toward the quantitative approach, aiming to avoid subjectivity and look at natural grouping [25]. Numerical soil taxonomy is used to create homogeneous, geographically distinct classes and reveal relationships between soil properties and landforms [21]. According to Deressa et al. [26], variability within and between profiles would be more pronounced by numerical classification. This classification approach would instead reinforce and consider pedogenetic processes [24]. In addition, assessing intra- and inter-profile similarity could improve the precision and accuracy of soil classification [27].

Numerical soil taxonomy employs metrics to calculate the distance among pairs of soil samples, and samples with a closer distance will be classified into the same soil class [28]. However, it may not always be easy to adhere to this system since many numerical soil classifications rely on distance metrics, which are not consistent as measures of classification uncertainty [29]. Accordingly, a given soil profile could be classified into more than one class at a time. It is also not always easy to visualize and interpret numerical soil taxonomy results [30]. On the other hand, Beaudette et al. [27] have devised an algorithm for quantitative pedology (apq) to overcome these limitations. A distance-based algorithm is then used to classify unknown samples into soil classes [31,32]. Numerical soil classification algorithms could also help identify soil classes and describe differences between soils [29,33].

The use of soil sequences is usually limited to studying soil processes where only one factor varies between sites, which makes it difficult to determine the defining soil-forming factors when several factors act simultaneously [34]. In this regard, employing appropriate multivariate analyses on soil attributes could reveal key environmental factors that govern spatial soil property distribution at the landscape scale [34,35]. Principal component analysis (PCA) and redundancy analysis are among the most commonly applied multivariate analyses for characterizing spatial soil property distribution [36]. PCA is used to explore the multivariate relationship between soil physicochemical properties and group these variables into a statistical factor that causes soil variability. The groups may then be used to establish relationships between soil properties and environmental factors [34,35], infer the underlying soil-forming processes [37,38], and generalize patterns of soil behavior in response to anthropogenic disturbance [29]. PCA provides a weighted distance matrix [31]. The most influential soil properties identified through PCA rotation represent a cluster and can be used to navigate soil taxonomy [39].

As the mechanisms and vectors of soil mixing, the homogenization of the soil caused by termites may not result in a clear textural change [40]. The nature of soil horizons could change, making it difficult to assign termite-mediated soils to ST or WRB soil classes. Since termite activities regulate pedogenesis and play a critical role depending on various soil conditions [41,42], it may be difficult to identify the key pedogenic processes in termite-mediated soils. This is because soil characterization through these systems assumes that pedogenic processes move vertically up or down, i.e., unidirectional. The previously limited research relating termite bioturbation to soil [43,44] was classified following the ST, WRB, or other classification systems. In these studies, the pedogenetic processes that form soils are neglected. Görres [45] also mentioned that soil features, which are generally surged by soil invertebrates, are often ignored in these soil taxonomies. In general, prior work in this area is limited, and at the time of undertaking the current study, only a few studies examined termite-mediated soil in the study area. A new suffix was adopted recently only by Salvucci et al. [46] to describe soil horizons formed by termite bioturbation, suggesting that further research is needed.

As termites usually inhabit degraded land in the study area and elsewhere in the world, accurate soil information is required to mitigate further land degradation [29,47]. The lack of accurate basic information on the pedogenic processes featured by termite bioturbation, topography, and land use limits an effort to address land degradation. On the other hand, as intrinsic termite bioturbation along with anthropogenic factors may lead the existing soil classification system in use to great uncertainty, allocating termite-mediated soils to a given soil class may raise the issue of reliability. Proper allocation of soil profiles into soil classes requires accurate identification of diagnostic characteristics, while few soil profile descriptions and some soil properties are measured where funds are limited. Thus, numerical classification as complementary to common soil taxonomy can improve allocation accuracy and enhance soil classification efficiency. However, quantitative soil classification has not been explored previously for termite-mediated soils, and the extent to which it differentiates the established soil classes is not known. Since termite-inhabited areas in southeast Ethiopia are characterized by gently undulating landscapes [1], several studies have highlighted the influence of topographic positions

at sub-watershed and watershed levels in the country [17,18,48]. On the other hand, while addressing soil spatial variability at the continent scale, a global soil classification system excludes topsoil variability and may only contribute a small amount to soil variability at the micrometer scale [49]. In this context, termite-induced fine-scale soil variability that proportionally expands with slope gradient needs further study, and this could be more adequately captured by a quantitative approach than the commonly used system. Knowledge of even subtle changes due to topography and bioturbation is critical to understanding soil heterogeneity at the landscape level [50].

Conversely, soil properties are vertically distributed within the soil profile according to management [51]. Though information on soil classification is inadequate to answer interdisciplinary questions, quantitative approaches require the expression of soil management effects on the properties of a particular soil type [52]. In this regard, pastoralists in the southeast area of the country own fragmented rangeland with few management practices [53,54]. Numerous studies have addressed the influence of land use on soil properties in Ethiopia [13,17,55]. However, the influence of rangeland use on termite activities and soil properties needs to be understood as land use changes continue to modify landscapes. Quantitative evidence on the heterogeneity of termite-affected soil properties through rangeland use and the effective depth to which erosion from the mound reaches has been largely unknown, and information is scanty for effective land use planning. According to Yao et al. [56], significant plant-soil property interactions occur in the top soils, particularly within 20–30 cm depth, due to different plant-soil system-related factors along the soil profile. Knowledge of soil properties under different land uses is important to determine soil characteristics, quality, and productivity [57]. Therefore, this study aimed to: (1) morphologically classify soil representing termite-inhibited areas at different topographical positions and quantitatively reclassify those soils; (2) describe the important pedogenic processes and physicochemical properties of soils that better describe and differentiate soil types; and (3) quantify the physicochemical properties of soil associated with different rangeland uses.

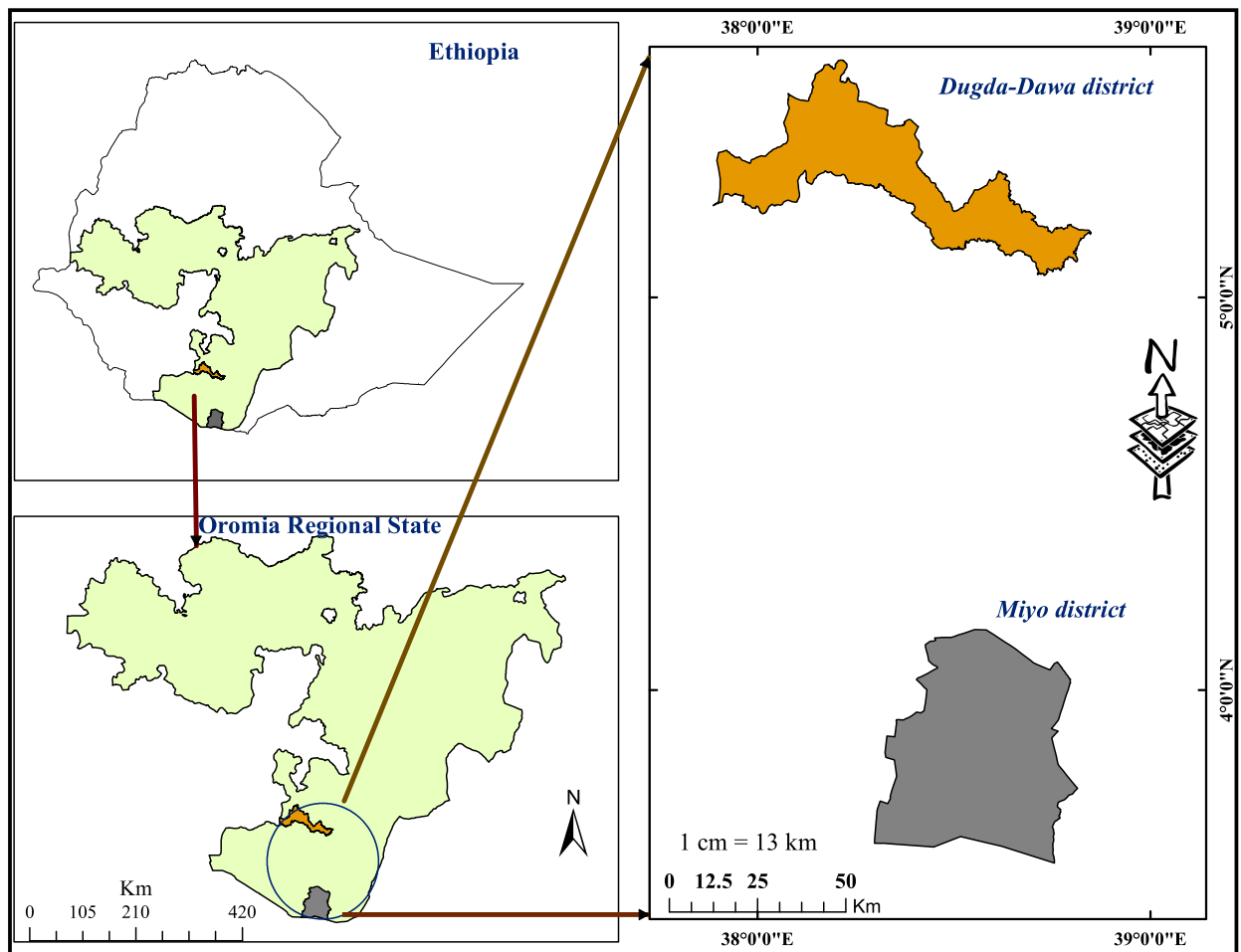


Fig. 1. Schematic map of study sites, *Dugda-Dawa* and *Miyo* districts, Ethiopia.

2. Materials and methods

2.1. Study area description

The study was conducted in two districts, namely *Dugda-Dawa* ($5^{\circ}22'46''$ to $5^{\circ}23'9''$ N and $38^{\circ}16'8''$ to $38^{\circ}16'10''$ E) and *Miyo* ($3^{\circ}33'34''$ to $3^{\circ}53'41''$ N and $38^{\circ}33'46''$ to $38^{\circ}35'27''$ E). Both districts are found in Oromia Regional State, Ethiopia (Fig. 1). The average altitude above sea level of these districts varies from 1305 to 1656 m. These areas are part of the southeast rangelands of Ethiopia and have hot and dry semiarid climates (BSh), according to the Köppen climate classification system [20]. Rangelands are characterized by bimodal precipitation, with 60% of rainfall occurring between March and May and 27% between September and November [58]. The 36-year (1983–2018) data from the National Meteorological Agency of Ethiopia showed that *Dugda-Dawa* receives a mean annual rainfall of 711 mm, while *Miyo* district receives 345 mm. The average annual temperature of the former area was 19.9°C and ranged from 13.3°C to 26.6°C , while the temperature in the latter area varied from 18.4°C to 29.5°C with an average value of 23.9°C . The geographical distribution of precipitation and temperature is prominent across the two areas; thereby, they are more variable in the *Miyo* district than in *Dugda-Dawa*. Savannah vegetation, containing a mixture of perennial herbaceous and woody plants, dominates the rangeland [58]. Quartzite and quartzitic sandstone are the geology of the underlying materials in *Dugda-Dawa*, whereas shales, sandstone, and limestone are the geology of the area in the *Miyo* district [58,59]. The general topography of the study area is typically a plain landscape with a slope gradient of $<10\%$.

2.2. Soil profile description

After a field survey, representative two-toposequences with widespread mounds, one in each district, were selected (Fig. 2). The toposequence in *Dugda-Dawa* is located at the *Ilala-Sara* site and differentiated into the summit, back slope, and toe slope, whereas the toposequence in *Miyo* is situated at the *Silala* site and identified as the foot slope and bottom slope. A total of five representative soil profiles, designated as Profiles 1 to 5, were excavated at different topographic positions. Profiles 1, 2, and 3 are located at the *Ilala-Sara* site in the *Dugda-Dawa* district, while Profiles 4 and 5 are found at the *Silala* site in the *Miyo* district. Profiles 1 and 2 were formed from weak and light red saprolites overlying quartz-diorite parent materials, in which coarse fragments dominated the overlying materials, and surface erosion was recurrently active around these soil profiles. Profile 3 was derived from alluvium deposits and near-seasonal stream channels. Profile 4 was formed from acid-forming eluvium residuum, while Profile 5 was developed from calcium carbonate-rich soils. All soil profiles were described *in situ*, and the volume of coarse fragments ($>2\text{ mm}$) was estimated in the field following the

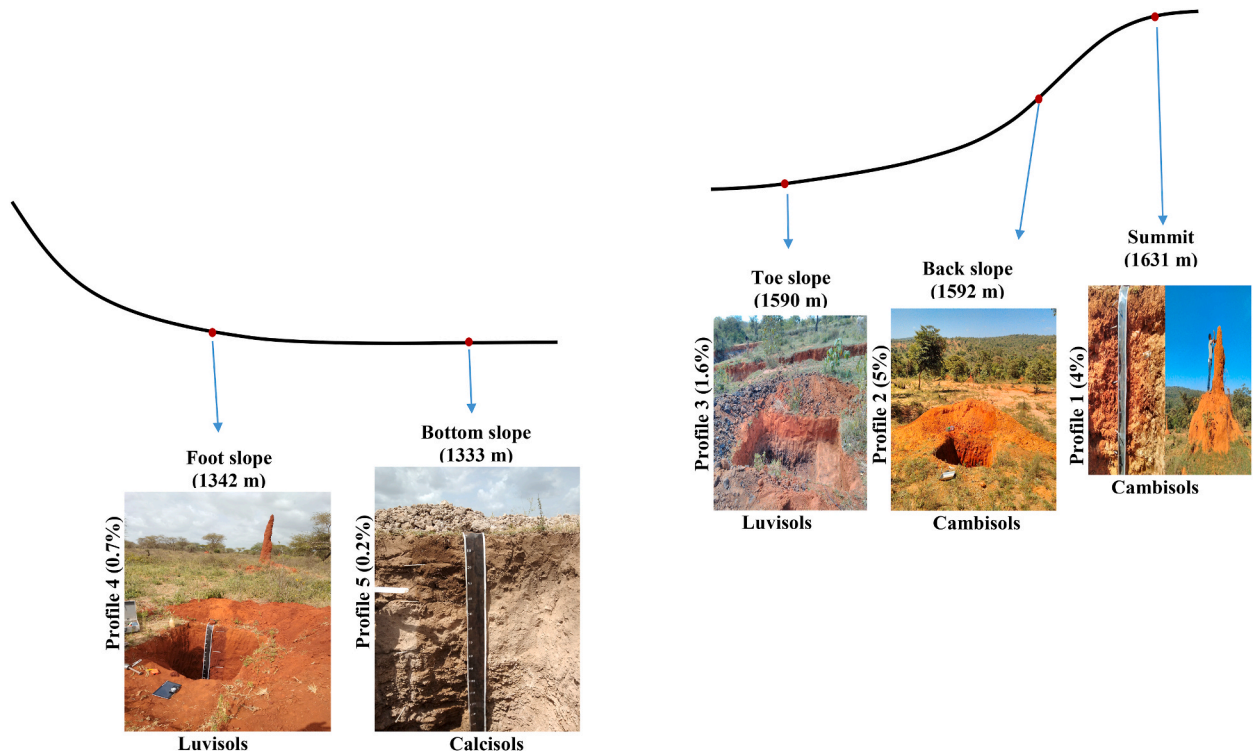


Fig. 2. Topographic map of the study toposequences along with soil profiles and corresponding termite mounds. Transect on the left and right show the toposequence at *Silala* in *Miyo* and *Ilala-Sara* in the *Dugda-Dawa* district, respectively. The number in the bracket indicates the average elevation of the topographical position above sea level.

Guidelines for Soil Description [60]. Genetic horizon-wise samples were collected from all soil profiles. Based on the field description and analysis of soil properties, the soil profiles were classified according to WRB [20]. All soil profiles were under open savanna used for extensive grazing.

2.3. Mound and soil sampling

To study the influence of termite bioturbation on soil properties across rangeland use, the summit position in *Dugda-Dawa* and a foot slope in *Miyo* district were stratified into enclosure, cultivated, and open-grazing land. Open-grazing land, which is commonly allocated for extensive cattle grazing, has a total surface area covered by <5% scattered grass and herbaceous vegetation. Cultivated land is mainly cropped with haricot beans and maize. The enclosure is mainly dominated by grasses and herbaceous vegetation, with the total surface area covered ranging from 15% to 65% and fenced for controlled grazing.

Since termite influence can be determined by the biogenic structures they form, the morphological properties of mounds were measured per rangeland use. The abundance of termite mounds was determined by counting the total number of mounds in each rangeland use and dividing by the area surveyed. Active mounds were opened, and representative soldier and worker castes were collected and preserved in 70% ethanol for genus-level identification. Accordingly, the genus *Macrotermes* dominates the study landscape except where *Odontotermes* are recognized in cultivated land at the foot slope position in the *Miyo* district. The mounds of these two genera were almost identical and showed cathedral shapes and a reddish-brown color.

Three active mounds per rangeland were selected and measured for height, basal diameter, volume, and mass of mounds. At each rangeland use, soil samples were obtained from three representative active mounds and their immediate adjacent soils. The samples from around the mounds were collected at a distance of 1.5 m from the base. The mound composite sample was collected at a depth of 30 cm after the entire mound soil was thoroughly mixed. The entire mound was considered because similar soil properties were observed within different parts of the mounds [61]. The soil immediately adjacent to the mound was sampled at depths of 0–10, 10–20, and 20–30 cm in a cardinal direction by centering the mound. The samples from four points of the same layer in the soil adjacent to the mound were thoroughly mixed to form a composite sample. A sampling depth of up to 30 cm was considered, assuming land management extends to this depth. This was also designed to maximize the effect of redistribution from mound erosion without necessarily sampling the nest and fungus garden. Furthermore, inadequate rainfall amounts do not detach particles from the mound and translocate them beyond this soil depth. In addition, a composite sample of reference control soil was taken for each mound. The corresponding reference control was located at a distance of 10 m from the mound, where evidence of termite influence is assumed to be limited. Other than genetic horizons, a composite soil sample was made from four subsamples, and all samples were collected in triplicate per rangeland use. The samples were separately tagged and transported.

2.4. Soil analysis

In the laboratory, soil samples were air-dried and sieved through a 2 mm sieve for soil physicochemical analysis, while a 0.5 mm sieve was used for organic carbon (OC) determination. Soil particle size analysis was determined by the hydrometer method [62]. The soil pH was determined in a 1:2.5 soil-to-water ratio (m/v) using a pH meter. Electrical conductivity (EC) was determined in the supernatant used for soil pH. Soil OC was determined following the Walkley-Black method [63]. The available phosphorus (Avail. P) content of the sample was determined by the Olsen method [64] and measured by a spectrophotometer at 882 nm. Cation exchange capacity (CEC) was determined by the ammonium saturation method [65], while exchangeable cations (Ca, Mg, K, and Na) were extracted by 1 M NH_4OAc at pH 7.0 [66]. Exchangeable Ca^{2+} and Mg^{2+} were measured using atomic absorption, while K^+ and Na^+ were measured with a flame photometer. The soil calcium carbonate equivalent (CCE) was determined using the trimetric method [67].

2.5. Data analysis

Cluster analysis was performed on PCA. PCA reduced multicollinearity and multidimensional quantitative soil properties [68]. Accordingly, more stable clustering was achieved [69]. In addition, PCA was also used to identify a few uncorrelated variables that summarize the overall variations. Cluster analysis was performed for two main goals: first, to understand the structure of natural grouping and compare the similarity of soil profiles through divisive clustering. Considering variability within a soil profile, a depth weighting dissimilarities of 0.01 was used, and then divisive hierarchical clustering (top-down approach) using the Diana function was used for soil profile comparison. This clustering approach successively splits the soil continuum into more homogeneous groups.

The second goal of clustering is to identify horizon groups using an agglomerative hierarchical approach, regardless of their magnitude. Agglomerative hierarchical clustering (bottom-up) considers each individual as a group and decides on the next closest similar group. In this approach, Euclidean distance on standardized data was used, and the most similar groups at each step were linked by the ward's minimum variance. To verify how faithfully a dendrogram preserves the original pair-wise distances, the linkage selection was assessed quantitatively through the cophenetic correlation and agglomerative coefficient [69]. According to Kassambara [69], the optimum number of clusters was determined by the silhouette width index. To understand the extent to which the obtained horizon groups reflect the natural groupings, the centroid (the average location of the horizon group) was calculated for every cluster, and the result was shown as the proximity of individual genetic horizons to the centroid on the clusters projected over the factor plane.

Both clustering methods were performed using selected soil profile parameters such as clay contents, soil pH, OC, CEC, Ca^{2+} , and Mg^{2+} . These soil variables are assumed to reflect soil development and are obtained through a multidimensional reduction technique.

Table 1
Morphological characteristics of the soil pedons along the toposequences in southeast Ethiopia.

Horizon	Depth (cm)	Horizon boundary	Munsell color notation		Soil structural units	Consistence				Rock fragment abundance, classification, and weathering
			Moist	Dry		Dry	Moist	Stickiness	Plasticity	
Pedon-1, located at the Summit, Dystric Skeletic Chromic Cambisols (Clayic, Cohesive, Humic, Isoptic, Saprolithic)										
A	0–12	Diffuse wavy	2.5 YR 3/4	2.5 YR 4/8	Weak medium crumbly	Soft	Very friable	Slightly sticky	Non-plastic	–
AB	12–30	Clear wavy	2.5 YR 3/6	2.5 YR 4/8	Weak coarse granular	Soft	Very friable	Slightly sticky	Slightly plastic	Very few, medium gravel, fresh or slightly weathered fragments
Bw	30–73	Clear wavy	2.5 YR 4/4	2.5 YR 4/6	Strong fine to coarse rock	Extremely hard	Extremely firm	Slightly sticky	Plastic	Many, coarse gravel and stones, fresh or slightly weathered fragments
BC	73–140	Gradual wavy	7.5 YR 4/6	7.5 R 5/6	Weak medium sub-angular blocky	Slightly hard	Extremely firm	Slightly sticky	Slightly plastic	Few, medium and coarse gravel, weathered fragments
Cr	140–200 ⁺		10 R 4/4	10 R 4/3	Weak very fine massive	Soft	Loose	Non-sticky	Non-plastic	–
Pedon-2, located at the back slope, Dystric Skeletic Chromic Cambisols (Clayic, Cohesive, Humic, Isoptic, Saprolithic)										
A	0–7	Gradual wavy	2.5 YR 4/4	2.5 YR 5/4	Weak very fine crumbly	Soft	Loose	Non-sticky	Non-plastic	Very few, fine gravel, fresh or slightly weathered fragments
AB	7–95	Clear wavy	2.5 YR 3/6	2.5 YR 4/8	Strong coarse rock	Hard	Very firm	Non-sticky	Slightly plastic	Abundant, coarse gravel and stones, fresh or slightly weathered fragments
Bw	95–140	Clear wavy	2.5 YR 4/8	2.5 YR 5/8	Weak fine angular blocky	Slightly hard	Friable	Slightly sticky	Slightly plastic	Few, fine and medium gravel, slightly weathered fragments
BC	140–170	Gradual wavy	2.5 YR 4/8	2.5 YR 5/8	Weak fine to medium angular blocky	Slightly hard	Very friable	Non-sticky	Slightly plastic	Very few, fine gravel, weathered fragments
Cr	170–200 ⁺		2.5 YR 5/8	2.5 YR 5/8	Weak fine massive	Soft	Friable	Non-sticky	Non-plastic	–
Pedon-3, located at the toe slope, Chromic Gleyic Luvisols (Clayic, Neocambic, Differentic, Dystric, Humic)										
A	0–10	Clear wavy	2.5 YR 4/4	2.5 YR 5/4	Weak medium sub-angular blocky	Soft	Loose	Slightly sticky	Non-plastic	–
AB	10–40	Clear wavy	2.5 YR 3/6	2.5 YR 4/8	Weak fine to medium sub-angular blocky	Soft	Loose	Non-sticky	Non-plastic	Very few, medium gravel, fresh or slightly weathered fragments
Bg	40–70	Abrupt smooth	7.5 YR 4/1	7.5 YR 5/3	Weak medium prismatic	Slightly hard	Very friable	Slightly sticky	Slightly plastic	–
Bt	70–200 ⁺		7.5 YR 3/1	7.5 YR 4/1	Moderate very coarse angular blocky	Hard	Firm	Very sticky	Very plastic	–
Pedon-4, located at the foot slope, Chromic Luvisols (Clayic, Dystric, Humic)										
A	0–10	Clear smooth	2.5 YR 4/4	2.5 YR 4/6	Moderate medium granular	Slightly hard	Very friable	Slightly sticky	Non-plastic	–
AB	10–55	Gradual smooth	10 R 3/6	10 R 4/6	Weak fine to medium sub-angular blocky	Slightly hard	Very friable	Slightly sticky	Slightly plastic	–
Bt	55–90	Gradual smooth	2.5 YR 5/4	2.5 YR 3/6	Weak fine to medium angular blocky	Slightly hard	Very friable	Slightly sticky	Slightly plastic	–
Bo	90–200 ⁺		2.5 YR 3/6	10 R 3/6	Weak coarse prismatic separated into	Hard	Friable	Slightly sticky	Slightly plastic	–

(continued on next page)

Table 1 (continued)

Horizon	Depth (cm)	Horizon boundary	Munsell color notation		Soil structural units	Consistence				Rock fragment abundance, classification, and weathering
			Moist	Dry		Dry	Moist	Stickiness	Plasticity	
moderate medium to coarse angular blocky										
<i>Pedon-5, located at the bottom slope, Skeletic Cambic Calcisols (Loamic, Humic, Isoptic)</i>										
Ak	0–18	Clear smooth	5 YR 4/2	7.5 YR 6/1	Weak fine to medium sub-angular blocky	Soft	Very friable	Slightly sticky	Plastic	–
AB	18–42	Clear smooth	2.5 YR 5/1	10 YR 5/2	Weak fine to medium sub-angular blocky	Soft	Loose	Slightly sticky	Slightly plastic	Common, coarse gravel, fresh or slightly weathered fragments
Bk	42–70	Clear smooth	5Y 6/1	5Y 8/1	Weak medium to coarse sub-angular blocky	Soft	Very friable	Slightly sticky	Slightly plastic	Very few, fine gravel, fresh or slightly weathered fragments
Ck	70–120	Gradual smooth	2.5Y 8/2	5Y 8/1	Strong coarse massive	Hard	Firm	Non-sticky	Non-plastic	Dominant, medium gravel, weathered fragments
Ckm	120–200 ⁺	–	2.5Y 7/1	5Y 8/1	Strong coarse massive	Hard	Firm	Non-sticky	Non-plastic	Dominant, coarse gravel, fresh or slightly weathered fragments

In addition, Munsell dry color and coarse fragments were added to visualize the difference in the standard soil profile. Finally, a comparison was made between the numerical and WRB soil classification systems. The quantitative numerical classification was implemented in R and RStudio (version i386 4.0.5) [70]. Agglomerative hierarchical clustering on PCA was performed through the FactoMineR package. The results were visualized using the factoextra package and graphically by a dendrogram. The *aqp* R package was used to perform divisive hierarchical clustering and visualization of the profile data.

A two-way repeated measure analysis of variance (ANOVA) was also performed to test the overall effects of rangeland use, where termite mounds and different depths were considered dependent factors while rangeland use was treated as an independent factor. The repeated measures aspect of the data makes it interesting because the assumption of independence may no longer be valid as observations on the mound and adjacent soil often exhibit correlation. The key assumptions of ANOVA—normality, homogeneity, and sphericity—were tested before analysis. With the violation of sphericity, an adjustment by the Greenhouse-Geisser correction was made for a significant variable. Using the Bonferroni multiple-testing correction method, significant differences among treatments were detected at the <0.05 probability level.

3. Results and discussion

3.1. Soil description

All identified profiles were very deep, and the morphological distinctness of each soil profile and associated horizon was concisely described (Table 1). The topsoil of the profiles was reddish-brown, which changed to red in the subsoil horizons, except for Profiles 3 and 5, which exhibited brown to dark gray and dark reddish gray to light gray soil colors, respectively. The soil structure was granular or crumbly at the surface that changed to weak, fine sub-angular blocky below the surface layers, moderate to strong sub-angular blocky, and massive in the subsoil horizons, while friable soil consistence became firm with soil depth.

Selected soil physicochemical properties of the profiles are presented in Table 2. The soil profiles were characterized by sandy clay loam, except for Profiles 1 and 2. The soil pH ranged from neutral to moderately acidic. However, Profile 5 had an alkaline soil reaction with a calcium carbonate content of 265 g kg⁻¹ at the surface that rapidly increased with depth and reached 565 g kg⁻¹ on the subsurface horizon. While Profiles 4 and 5 had moderate OC content, it was low in the other soils. Profile 3 showed distinct high clay, CEC, Ca²⁺, and Mg²⁺ contents on the lowermost horizon. Exchangeable Ca²⁺ and Mg²⁺ were irregularly enhanced with soil depth in Profiles 1 and 4, while both cations gradually decreased in Profile 2. The Ca²⁺ content was gradually decreased, whereas the Mg²⁺ content was irregularly increased with depth in Profile 5.

3.2. WRB soil classification

The classification of the soils following WRB showed that the subsurface soils of Profiles 1 and 2 met the requirements of the cambic horizon identified by horizon thickness, texture, red hues, and high chroma. Below these cambic horizons, the soil of Profiles 1 and 2 also exhibited the properties of a cohesic horizon [20]. Thus, the landscape comprised Dystric Skeletic Chromic Cambisols (Clayic, Cohesic, Humic, Isoptic, Saprolithic) at the summit (Profile 1) and back slope (Profile 2) positions. The subsurface horizons of

Table 2
Physicochemical properties of the soil pedons along toposequences in southeast Ethiopia.

Horizons	Sampling depth (cm)	Sand (>63 μm)	Silt (2–63 μm)	Clay (<2 μm)	Texture class	CCE (g kg^{-1})	pH (1:2.5H ₂ O)	EC (dS m^{-1})	OC (g kg^{-1})	Avail. P (mg kg^{-1})	cmol _c kg^{-1}				
											g kg^{-1} of fine earth				
Pedon-1, located at the Summit, Dystric Skeletic Chromic Cambisols (Clayic, Cohesive, Humic, Isoptic, Saprolithic)															
A	0–12	680	60	260	Sandy clay loam		5.7	1.5	12.5	4.8	5.2	0.5	0.4	0.19	0.1
AB	12–30	500	80	420	Sandy clay		6.0	1.8	13.3	4.3	10.0	0.9	0.8	0.19	0.1
Bw	30–73	440	120	440	Clay		5.5	1.3	11.7	9.2	10.6	0.7	0.5	0.16	0.1
BC	73–140	510	130	360	Sandy clay		5.9	1.3	8.8	8.62	9.0	1.4	0.5	0.26	0.1
Cr	140–200 ⁺	720	140	140	Sandy loam		6.1	2.0	6.6	5.6	6.0	1.0	0.8	0.27	0.1
Pedon-2, located at the back slope, Dystric Skeletic Chromic Cambisols (Clayic, Cohesive, Humic, Isoptic, Saprolithic)															
A	0–7	780	80	140	Sandy loam		5.7	0.9	11.7	7.9	5.2	1.7	0.5	0.11	0.2
AB	7–95	580	80	340	Sandy clay loam		5.2	0.8	11.7	6.7	7.6	1.2	0.6	0.15	0.2
Bw	95–140	360	20	620	Clay		6.0	1.1	9.8	6.5	4.8	1.4	0.5	0.12	0.2
BC	140–170	480	60	460	Sandy clay		5.4	0.7	2.3	6.7	9.2	1.2	0.7	0.16	0.1
Cr	170–200 ⁺	540	100	360	Sandy clay		5.1	0.6	3.9	6.4	8.6	1.3	0.5	0.19	0.1
Pedon-3, located at the toe slope, Chromic Gleyic Luvisols (Clayic, Neocambic, Differentic, Dystric, Humic)															
A	0–10	740	40	220	Sandy clay loam		5.8	1.2	12.5	6.4	7.8	1.8	1.1	0.38	0.1
AB	10–40	740	40	220	Sandy clay loam		5.7	0.9	10.5	9.2	6.2	1.7	1.1	0.21	0.1
Bg	40–70	660	100	240	Sandy clay loam		5.6	0.6	11.7	12.4	7.2	1.2	0.9	0.29	0.1
Bt	70–200 ⁺	340	140	520	Clay		6.0	1.3	9.4	10.7	26.4	12.2	3.2	0.22	0.2
Pedon-4, located at the foot slope, Chromic Luvisols (Clayic, Dystric, Humic)															
A	0–10	580	200	220	Sandy clay loam		6.7	2.1	16.4	5.0	9.2	3.9	0.3	0.18	0.2
AB	10–55	520	100	380	Sandy clay		6.0	0.8	12.1	3.2	9.8	2.4	0.3	0.15	0.1
Bt	55–90	380	140	480	Clay		6.4	0.8	7.8	2.8	14.2	4.4	1.3	0.17	0.2
Bo	90–200 ⁺	480	260	260	Sandy clay loam		7.2	2.3	7.8	4.4	17.4	5.5	1.7	0.15	0.1
Pedon-5, located at the bottom slope, Skeletic Cambic Calcisols (Loamic, Humic, Isoptic)															
Ak	0–18	480	260	260	Sandy clay loam	265	7.6	3.7	23.4	5.8	14.2	51.1	1.5	0.15	0.1
AB	18–42	560	220	220	Sandy clay loam	525	7.4	3.8	19.5	6.9	10.0	51.5	0.7	0.17	0.2
Bk	42–70	480	240	280	Sandy clay loam	685	7.6	3.8	13.7	8.8	9.4	54.7	1.7	0.15	0.1
Ck	70–120	550	150	300	Sandy clay loam	680	7.8	4.0	14.4	9.6	8.2	47.1	4.5	0.15	0.1
Ckm	120–200 ⁺	740	40	220	Sandy clay loam	565	8.2	6.4	13.7	4.7	16.4	31.5	4.8	0.10	0.1

CCE: Calcium Carbonate Equivalent; CEC: Cation Exchangeable Capacity; EC: Electrical Conductivity; OC: Organic Carbon.

Profiles 3 and 4 fulfilled the diagnostic criteria of the argic horizon. Argic horizons having a CEC of clay greater than $24 \text{ cmol}_c \text{ kg}^{-1}$ and high base saturation qualified the soils at the toe slope (Profile 3) and foot slope (Profile 4) for Gleyic Chromic Luvisols (Clayic, Neocambic, Differentic, Dystric, Humic) and Chromic Luvisols (Clayic, Dystric, Humic), respectively. The CCE in the subsurface of Profile 5 was higher than 15 %, which qualified the diagnostic criterion of the calcic horizon, and thus, Skeletic Cambic Calcisols (Loamic, Humic, Isoptric) occurred on the bottom slope.

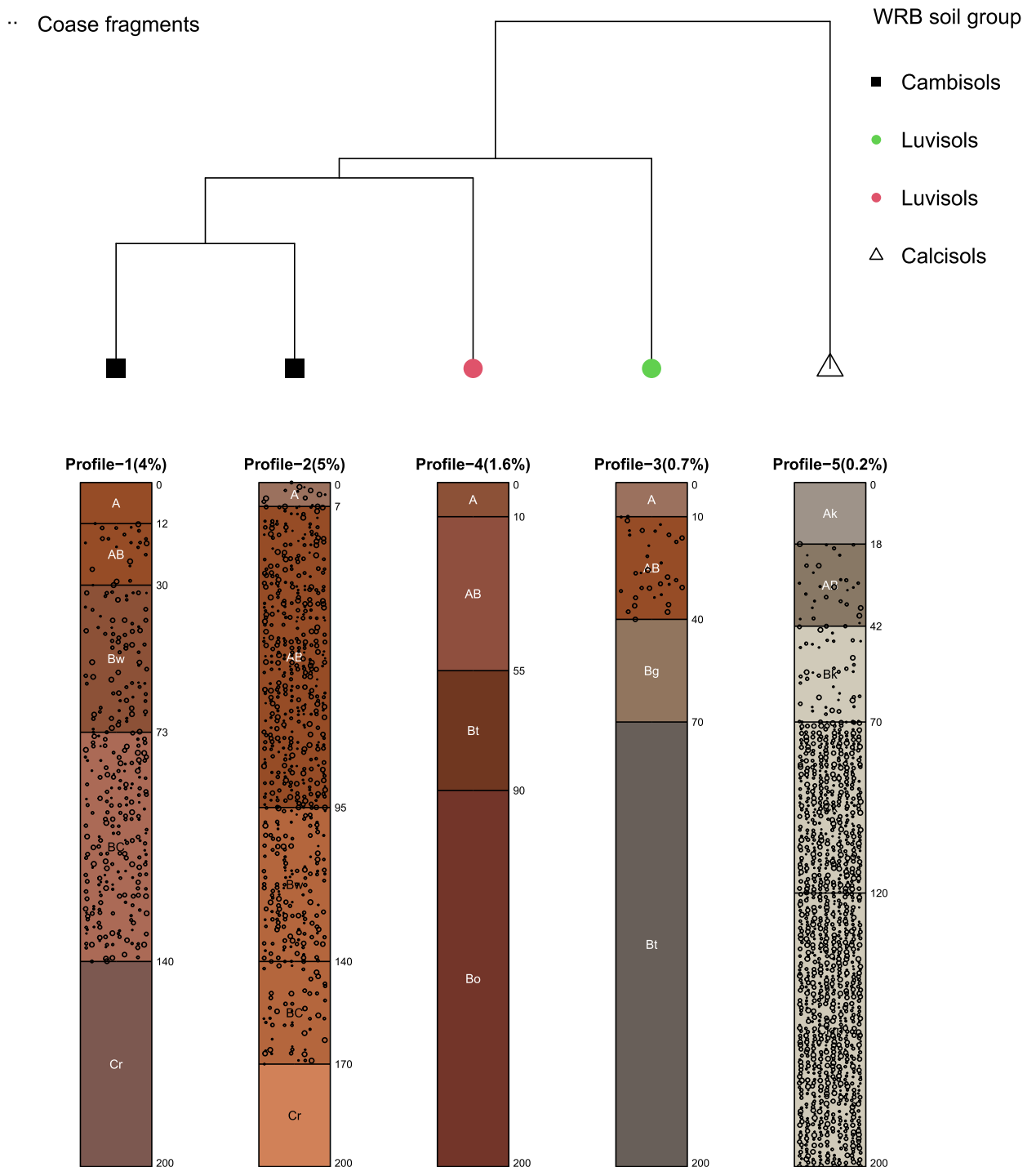


Fig. 3. Divisive clustering and standard soil profile sketch with horizon label and depth (cm), dry Munsell soil color, percent coarse fragments, profile ID with slope gradient in a bracket, and WRB soil groups. (For interpretation of the references to color in this figure legend, the reader is referred to the Web version of this article.)

3.3. Numerical soil classification

Divisive hierarchical clustering showed the differentiation of soil profiles (Fig. 3). All profiles were segregated into three soil groups at a higher level. The first cluster represented the Cambisols located on the summit and back slope (Profiles 1 and 2). The second cluster identified Luvisols on the foot slope (Profile 4) and toe slope (Profile 3) that were fused to the first cluster. The third cluster signified the outlier Profile 5 (Calcisols) on the bottom slope that arbitrarily joined the other groups at a higher distance. The pairwise dissimilarity matrix results showed that Profiles 1 and 2 were similar by more than 80% (appendix). Profile 4 was similar to Profiles 1 and 2 by 78 and 69%, respectively. Profile 3 was also similar by 67, 71, and 63% to Profiles 1, 2, and 4, respectively. Profile 1 tended to be stony, but with less gravel than Profile 2, while Profile 3 was almost gravel-free, except for the very few fresh or slightly weathered medium gravels found near the surface (Table 1). The gravelly horizons were exposed in Profile 2, while the gravelly horizons of Profile 1 were covered by a thick, gravel-free horizon. On the other hand, fresh or slightly weathered, common to dominant coarse gravels exceeding 80% were particularly common in the lower soil horizons of Profile 5, while Profile 4 was gravel-free throughout the profile depth.

Cambisols of Profiles 1 and 2 were similar in terms of soil pH, CEC, Mg^{2+} , and Ca^{2+} contents. Pinheiro et al. [47] reported the similarity among soil profiles based on common characteristics, while high calcium content separated the soil types. Hughes et al. [39] also reported similarities between different soil groups concerning soil pH, BS, CEC, and ESP, while the groups showed different distribution patterns with depth for other soil properties. These Cambisols were also exposed to erosion and dominated by gravelly layers. Accordingly, the degree of slope inclination and the extent of termite bioturbation probably resulted in a slight difference.

In addition to environmental differences, Luvisols on the toe slope (Profile 3) had clay synthesis at the subsurface horizon and received soil materials eroded from the summit and back slope, which differentiated this profile from Luvisols on the foot slope (Profile 4). As described by Labaz et al. [71], the proportion of particle-size altered in subsoil due to clay translocation and its accumulation in the illuvial horizons makes a distinction in Luvisols. The Luvisols at the foot slope (Profile 4) have morphological similarities to truncated Cambisols (Profiles 1 and 2). However, relatively well-expressed polyhedral soil structure and substantial iron oxides as 2.5 YR 3/6 suggest that ferrihydrite and hematite are relatively important iron oxide phases [72], and intermediate CEC values probably set them apart Profile 4 from Profiles 1 and 2. Cambisols were differentiated from Luvisols (Profile 3) by high sand, low silt, and moderate to high levels of clay content, which are consistent with previous studies by Dinssa and Elias [73].

On the other hand, the dominance of calcium carbonate distinguished Calcisols (Profile 5) from Cambisols or Luvisols in addition to high Ca^{2+} , pH, Mg^{2+} , and OC in the soil. This soil profile was formed from a lacustrine deposit that generally had a grayish color and displayed other distinguishable features from those of the other soil profiles.

The soil profile groupings suggested by the divisive clustering method approximate the soil classification obtained by the WRB classification system. In line with this result, Deressa et al. [26] also observed the strong similarity of numerically classified soils to WRB and ST-classified soils. Young and Hammer [21] reported that agreement between numerical and non-numerical classifications could be enhanced when a comparison was made by textural classes. In our study, quantitative classification focused on clay, pH, OC, CEC, Ca^{2+} , and Mg^{2+} contents could result in a similar soil grouping as that of the WRB classification system.

3.4. Pedological processes

Principal component analysis allocated the soil profile properties to two distinguishable groups (Fig. 4). The first dimension explained 50% of the variability, relating to soil pH, Ca^{2+} , OC, and Mg^{2+} . According to Oliveira et al. [74], the variables that form the first factor explain the highest percentage of variations and have the largest contributions to changes in soil characteristics. The second dimension captured 25.2% of the variability and highlighted the positive contribution of CEC and the clay contents of the studied soils.

Agglomerative hierarchical clustering differentiated the genetic horizons into three groups, as shown in the dendrogram (Fig. 5).

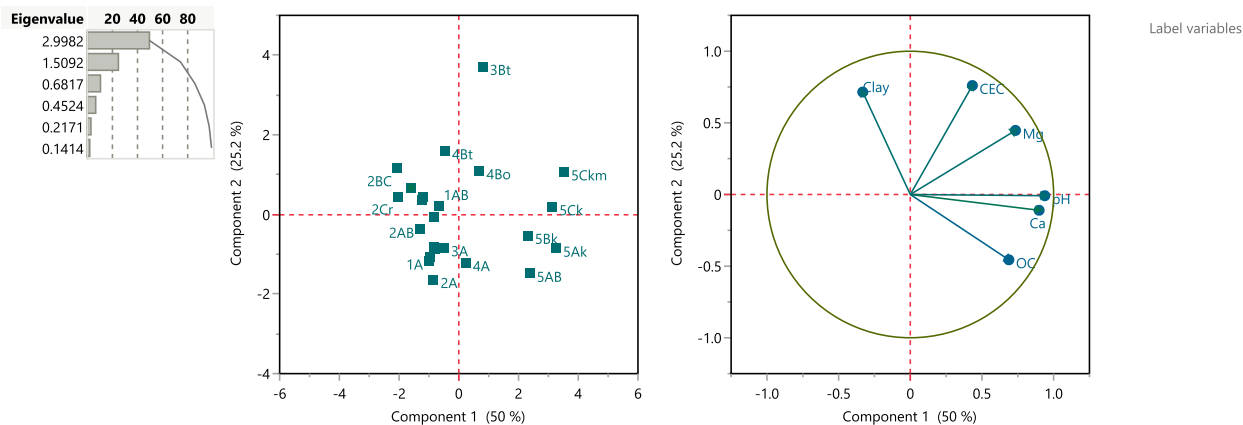


Fig. 4. The scree, component, and correlation plots show the relative importance of principal components in explaining the total variability of soil variables. (Explanation: the number designates the profile ID, and the letters indicate the horizon designation).

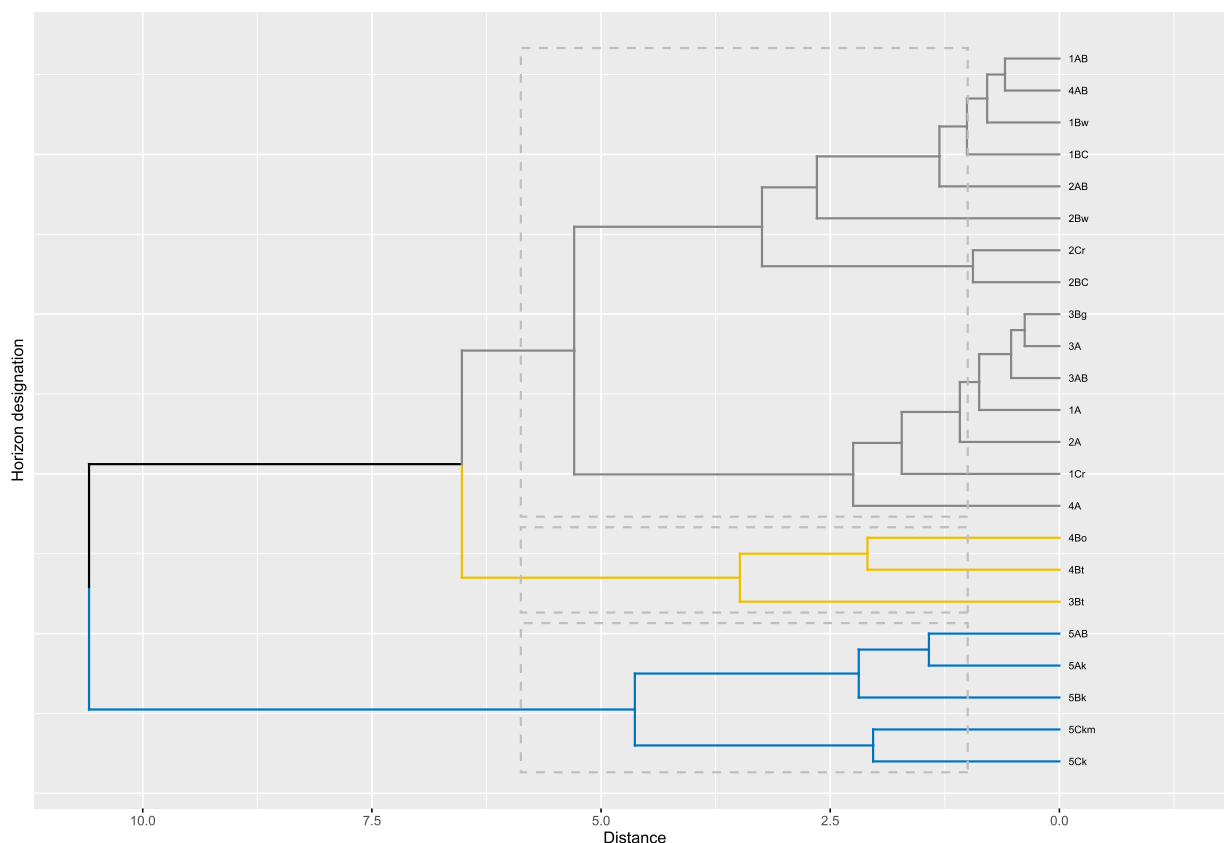


Fig. 5. Dendrogram for genetic horizon similarity based on quantitative soil parameters reflecting soil pedogenesis. (Explanation: the number designates the profile ID, and the letters indicate the horizon designation).

Starting at the top of the figure, the first cluster mainly comprised transitional horizons and slightly developed B horizons in Profiles 1, 2, and 4. This cluster also consisted of seven horizons, including the majority of the surface A-horizons, as well as the AB and Bg horizons of Profile 3 and the Cr horizons of Profiles 1 and 2. Within Cluster 1, the AB horizon of Profile 2 was more similar to the AB horizons of Profiles 1 and 4 than the AB horizon of Profile 3. The relatively similar BC, Cr, and Bw horizons of Profile 2 were associated with the first group at a higher connection level. In the first cluster, the A, AB, and Bg horizons of Profile 3 were also more similar than the others.

The distribution of individual genetic horizons projected over the factor map and the clustering of horizons are presented in Fig. 6 (detailed analyses are given in the appendix). In this plot, the distance of each horizon differs from the average group within a cluster. The closeness of a horizon to the centroid of each cluster gives insight into the representativeness of the horizons in the group. In a previous study, Teng et al. [75] also treated the shortest distance of a centroid as the best match between the Australian soil classification order and FAO soil units. According to these authors, the closeness of soil horizons gives insight into the pedological similarities between classes. Accordingly, the group of surface horizons and most transitional horizons in the first cluster were distinguished on the first factorial axis. Sequentially, the most representative horizons were AB of Profile 2, AB of Profile 4, Bg and AB of Profile 3, and the AB horizon of Profile 1. The soil variables that described the soil horizons in the first cluster were low in pH, CEC, Ca^{2+} , and Mg^{2+} contents (appendix). The representative AB horizons in the first cluster may reflect termite-induced limited OC content mixed in the surface soil. In addition to the Isoptic supplementary qualifier [20], termite footprints could be reflected by granular, crumbly, or weak fine to medium sub-angular blocky structures and gradual to diffuse horizon boundaries [1] for all profiles, except for the soil at the toe slope. The second-best representative Bg horizon of Profile 3 in the first cluster probably indicated gleization due to cyclic oxidation and reduction processes, which favored the hydrolysis of primary minerals and enhanced clay formation. According to Bonifacio et al. [76], the evidence of *gleyic* properties suggests intensive mineral weathering in the soil. The similarity between the A, AB, and Bg horizons of Profile 3 is probably related to the upward movement of certain salts due to capillary rise following seasonal water fluctuations. The similarity between AB horizons in Profiles 1 and 4 may indicate comparable pedogenic processes at different topographical positions. Similar observations were reported by Deressa et al. [26], indicating comparable pedogenetic processes at different landscape locations. The low pH, CEC, Ca^{2+} , and Mg^{2+} values that separated the first cluster and the representative horizons in this group reflected weak horizon development that mainly formed cambic horizons. Furthermore, the clustering of horizons in

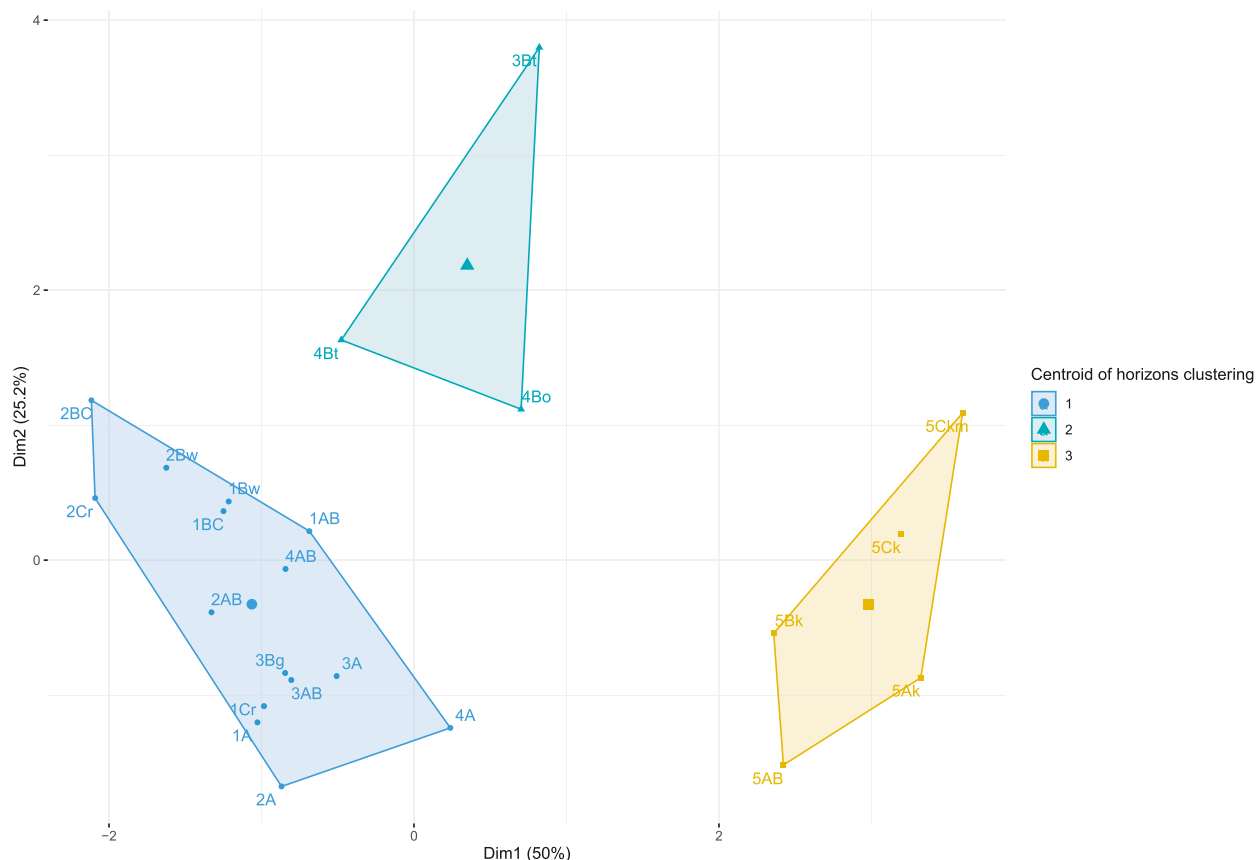


Fig. 6. The most representative horizons with centroids of each cluster projected over the first (Dim1) and second (Dim2) factor planes of the leading two principal components. (Explanation: the number designates the profile ID, and the letters indicate the horizon designation).

Profile 3 into the same group with horizons in Profiles 1 and 2 indicates the downslope translocation of soil materials from the upslope and deposition at the toe slope position.

The second cluster consists of the Bt and Bo horizons of Profiles 3 and 4 (Fig. 5). At the second level, the outlier horizon, the Bt horizon of Profile 3, was fused rather arbitrarily at a much higher distance to the more similar Bt and Bo horizons of Profile 4. The horizons that formed the second cluster were differentiated on the second factorial axis (Fig. 6). This group of horizons was homogeneous, but the most representative of the cluster was the Bt horizon in Profile 4. The second cluster was more explained by clay and CEC (Fig. 4). Horizon grouping in the second cluster probably substantiated significant clay accumulation in the subsurface. Following clay accumulation, high CEC was described the most in this group. In this cluster, the most representative Bt horizon of Profile 4 reveals clay eluviation-illuviation processes in the soil. The next representative Bo horizon probably indicates the residual accumulation of sesquioxides after intense weathering. Apart from illuviation processes, the least representative Bt horizon in Profile 3 and its less similarity to the second cluster probably indicate clay synthesis.

The third cluster had only horizons from Profile 5 (Fig. 5). In the third cluster, the Bk horizon from Profile 5 is distinctly joined by the more similar Ak and AB, as well as the Ck and Ckm horizons. In contrast to the former two clusters, the group of horizons in Profile 5 was well isolated on the first factorial axis (Fig. 6). The most representative horizon of this group was Bk, while Ckm was the least representative. In contrast to the first cluster, the third cluster was defined by high Ca^{2+} , pH, Mg^{2+} , and OC (appendix). The grouping of horizons into the third cluster substantiated the calcification processes in Profile 5. This process formed calcium carbonate in particular and was depicted by the most representative Bk horizon that qualified as a calcic horizon. The second most representative Ck horizon and the similarity between this and Ckm horizons in Profile 5 could be related to the petrocalcic horizon, whereas the similarity between Ak and AB in this profile reveals carbonate accumulation in the surface soil. Pinheiro et al. [47] reported a high probability of the occurrence of Cv horizon to identify vertic property. Labaz et al. [71] also reported a statistical comparison showing a high similarity between C and Ck for three different soil profiles studied along a catena. The grouping of soil horizons in the same cluster, particularly the first two clusters, suggests that quantitative classification is attractive in describing un-sampled termite-mediated soils where soil heterogeneity is important. The WRB soil classification system, however, is limited in its ability to provide such information.

3.5. Mound morphology and abundance

At the summit position in *Dugda-Dawa*, the termite mounds had an average height of 3.6 m under the enclosure and 4.7 m in open-grazing land, with an abundance of 4 and 19 mounds ha^{-1} , respectively (Table 3). Under cultivated land at this position, termite mounds had a height of 1.7 m and an abundance of 22 mounds ha^{-1} . At the foot slope in the *Miyo* district, termite mounds reached 4.5 m in the enclosure while they were about 3.2 and 5.3 m in open-grazing and cultivated land, respectively. Termite mound abundance per ha was 7 in the enclosure and 12 in open-grazing, while it was about 18 mounds in cultivated land on a foot slope in the *Miyo* district. For rangeland use at the summit, the mean basal diameter and volume of mounds were 3.4 m and 11 m^3 in the enclosure, 3.2 m and 12.5 m^3 in open-grazing, and 4.9 m and 10.4 m^3 in cultivated land, respectively. The average basal diameter of mounds on the foot slope was about 2.4 m in the enclosure, 1.8 m in open-grazing land, and about 2.8 m in cultivated land, while the average volume of mounds under these rangeland uses was 6.8, 2.6, and 10.9 m^3 , respectively.

Several studies have mentioned the strong association between land use and termite communities. This indicates the influence on biogenic structures is likely due to changes in termite habitats following anthropogenic disturbance [77–79]. The results in Table 3 are in contrast to Bera et al. [80], who reported that the height, masses, density, and regeneration rate of termite mounds increased with vegetation density in the order of grassland, dispersed, and dense vegetation. This discrepancy might be explained as certain land use practices affect the abundance and richness of termite communities, which could lead to the loss of functional groups in some cases [15,81]. According to Anyango et al. [77], the abundance, occurrence, diversity, and foraging activities of termites also depend on soil depth, available feeding types, soil moisture, cropping season, and environmental location.

3.6. Termite bioturbation effects

Soil particles varied significantly, except for silt content resulting from rangeland use ($F = 2.0, p > 0.05$) (Table 4). Sand content was significantly higher in enclosures and cultivated land than in open-grazing land. In contrast, clay particles were higher in open-grazing land soils than in enclosures and cultivated land. Sand content was lower, and silt and clay contents were higher on mounds than on the respective control soil. However, clay content was comparable between mounds and control soil under cultivated and open-grazing land. In the soil adjacent to mounds, significant differences in soil particles were not observed along soil depth, although sand content decreased across soil depths in open-grazing land.

Relatively high sand content in the enclosure and cultivated land is in contrast to Negasa et al. [13], who reported high sand content in grazing land but low sand content in cultivated land due to intensive soil management. The high clay particles in open-grazing soil may be related to the clay-enriched horizon caused by saprolite underlying the soil, as in the case of the summit, and the enriched fine particles at the foot slope. In this regard, Damene et al. [82] indicated low sand and comparable clay contents in open-grazing land in contrast to enclosure land. An increase in silt and clay contents in mounds could be due to termites preference for fine particles [83]. Comparable clay content between mound and control soils across rangeland use is probably due to the lower selection of termites for fine particles with a higher clay content in the reference soil and vice versa [42]. The decreasing sand contents with depth are in line with the observation by Negasa et al. [13], and the absence of a significant depth difference is probably due to erosion from the mounds.

Soil pH was significantly affected by rangeland use ($F = 6.5, p < 0.01$) and termite bioturbation ($F = 10.2, p < 0.001$). Open-grazing land had the lowest pH value compared to enclosure and cultivated land (Table 4). Termite mounds had comparable soil pH values to the corresponding control soil. In addition, the pH did not differ across depths in the soil adjacent to the mounds. Soil EC value was significantly affected by rangeland use ($F = 27.0, p < 0.01$) and termite bioturbation ($F = 30.5, p < 0.001$). Open-grazing land had the highest EC value compared to enclosures and cultivated land. Termite mounds had an eight-to thirteen-fold higher EC than the corresponding control soils, and the magnitude of the increase was more prominent in the enclosure than under cultivated and open-grazing land. However, the EC values did not differ significantly across depths in the soil adjacent to the mounds. Rangeland use and termite bioturbation had significant ($p < 0.01$ and $p < 0.001$, respectively) effects on soil OC (Table 4). While OC was comparable between mounds and the soil adjacent to the mounds, the content in termite mounds was higher by 44, 20, and 45% than the content in control soil under enclosure, cultivated, and open-grazing land, respectively. Rangeland use and termite bioturbation had significant ($p < 0.001$ and $p < 0.001$, respectively) influences on available P. The available P content of the soil under the enclosure and cultivated land was lower than that of open-grazing land by 43 and 21%, respectively. The available P content of termite mounds was higher than that of control soil by 23–111%. In general, termite mounds and the respective adjacent soil did not significantly differ in available P content. However, the average value in mounds was lower than that of the adjacent soil under the enclosure.

Table 3
Characteristics of termite mounds across rangeland use in *Dugda-Dawa* and *Miyo* districts.

Positions	Rangeland uses	Density (ha^{-1})	Height (m)	Basal diameter (m)	Volume (m^{-3} mound $^{-1}$)	Soil mass (t mound $^{-1}$)
Summit	Enclosure	4	3.6	3.4	11.0	14.7
	Open grazing	19	4.7	3.2	12.5	13.9
	Cultivated	22	1.7	4.9	10.4	16.8
Foot slope	Enclosure	7	4.5	2.4	6.8	9.1
	Open grazing	12	3.2	3.5	2.6	14.6
	Cultivated	18	5.3	2.8	10.9	3.0

Table 4

Physicochemical properties in termite-mediated soils across rangeland use in the study area.

Rangeland uses	Sampling units	Sand	Silt	Clay	pH, 1:2.5H ₂ O	EC, dS m ⁻¹	OC, g kg ⁻¹	Avail. P, mg kg ⁻¹	CEC				
		g kg ⁻¹							Cmol _c kg ⁻¹				
Enclosure	Mounds	500 b	173a	327a	6.8 b	15.8a	19.7a	5.9a	31.4a	10.5a	1.2a	0.19a	0.06
	0–10 cm	623a	113 b	263 ab	7.1a	1.0 b	23.0a	6.6 ab	25.5 b	5.6 b	0.5a	0.09 b	0.05
	10–20 cm	597a	110 b	293 ab	7.2a	0.9 b	22.0a	6.5 b	27.9 ab	7.1 b	0.5a	0.10 b	0.08
	20–30 cm	575a	98 b	327a	7.1 ab	0.5 b	21.8a	6.6 b	28.0 ab	7.1 b	0.6a	0.10 b	0.05
	Control	575a	130 b	261 b	6.2 b	1.2 b	13.7 b	4.8c	7.5c	2.4c	0.3 b	0.13 b	0.06
	Mean ^a	581a	125	294b	6.9a	3.9b	20.0a	6.1c	24.0	6.5	0.6	0.12b	0.06b
Cultivated	Mounds	473 b	153a	373a	6.5 b	12.5a	19.6a	8.7a	25.1a	12.5a	0.4a	0.22a	0.06
	0–10 cm	623a	112 b	265 ab	7.0a	0.8 b	24.4a	7.4 ab	21.7 b	8.9 b	0.8a	0.12 b	0.05
	10–20 cm	583a	118 b	298 ab	7.1a	0.8 b	21.2a	7.3 b	21.6 ab	7.4 b	0.8a	0.10 b	0.07
	20–30 cm	595a	108 b	297 ab	7.1 ab	1.4 b	20.7a	7.2 b	21.8 ab	7.5 b	0.6a	0.11 b	0.08
	Control	656a	100 b	244 ab	6.1 b	1.3 b	16.4 b	5.3c	7.3c	1.5c	0.2 b	0.17 b	0.08
	Mean ^a	586a	118	295b	6.8a	3.4b	20.5a	7.2b	19.5	7.6	0.6	0.15 ab	0.07b
Open-grazing lands	Mounds	490 b	153a	357a	6.5 b	13.6a	19.3a	11.2a	30.8a	7.6a	0.8a	0.18a	0.14
	0–10 cm	520a	150 b	330 b	6.7a	5.3 b	19.2a	10.4 ab	29.6 b	5.1 b	0.5a	0.15 b	0.11
	10–20 cm	513a	135 b	352 ab	6.5a	9.2 ab	20.9a	8.6 b	30.1 ab	5.9 b	0.7a	0.16 b	0.10
	20–30 cm	493 b	140 b	367 ab	6.3 ab	11.0 ab	19.4a	8.1 b	30.7 ab	5.7 b	0.7a	0.15 b	0.09
	Control	533a	125 b	342 ab	6.1 b	1.6c	13.3 b	5.3c	7.2c	2.2c	0.2 b	0.15 b	0.07
	Mean ^a	510b	141	349a	6.4b	8.2a	18.4b	8.7a	25.7	5.3	0.6	0.16a	0.10a
F-Values	Bioturbation (F _{4, 20})	6.5*	6.1***	4.3**	10.2***	30.5***	10.8***	19.6***	145.7***	12.7***	14.1***	9.7**	2.2ns
	Rangeland (F _{2, 10})	5.7*	2.0ns	7.6*	6.5**	27.0**	6.5**	19.1***	3.1ns	1.4ns	1.4ns	7.1*	16.9***
CV (%)		14.3	30.5	21.7	6.3	99.5	22.6	21.7	22.3	69.3	52.8	36.6	34.8

CEC: Cation Exchangeable Capacity; EC: Electrical Conductivity; OC: Organic Carbon.

Ns: non-significant, *, ** and ***: significant at $\alpha = 0.05, 0.01$ and 0.001 probability level, respectively. Means followed by the same letter do not significantly different from each other.^a The average values of termite-mediated soils per sampling units taken to compare rangeland uses.

Cation exchange capacity, Ca^{2+} , and Mg^{2+} were significantly influenced only by termite bioturbation. While K^+ was affected by both factors, Na^+ was influenced only by rangeland use ($F = 16.9, p < 0.001$). Termite bioturbation improved the CEC, Ca^{2+} , and Mg^{2+} contents of mounds by three to eightfold over control soils. High K^+ and Na^+ values were observed under open-grazing land rather than in the enclosure or cultivated land, while CEC and basic cations were comparable between mounds and the soil adjacent to the mounds.

The lower soil pH values in open-grazing land than in enclosures and cultivated land are probably attributed to the higher rate of OM oxidation due to the high termite activity on open-grazing land, which produces organic acids and releases H-ions into soil solutions. The reduction of soil pH values under open-grazing land could also be related to the depletion of basic cations through surface erosion [17,18]. Comparable soil pH values between mounds and the soil adjacent to the mounds could be due to the accumulation of cations through erosion from the mounds. The findings agree well with the results of Bera et al. [80]. The higher EC values were recorded in the mound soils, which are probably associated with an enrichment of basic cations, particularly Ca^{2+} , corroborating the findings of Chisanga et al. [84]. On the other hand, some termite groups, such as the genera in this study, host atmospheric-fixing nitrogen bacteria [85,86]. According to Seymour et al. [87], in neutral to alkaline soil reactions, nitrate is the dominant form of N, and a large termite mound contains sixty-fold more nitrate than a reference soil. An increase in nitrate concentrations in the anion fraction of termite mounds suggests mineralization of OM, which elevated the EC content in the mounds [88]. The result on available P is in contrast to the study of Cheng et al. [89], which indicated increased available P content from farmland to forest or grassland. The higher available P in the mounds than in the adjacent soil could be due to the accumulation of litter for many years that led to humification and increased phosphorus release. Significantly higher divalent cations in the mounds and their adjacent soil than in the corresponding control soil, probably due to the role of these cations, particularly Ca, in soil structural stability against mound cracks. This is because soil shrinkage during the dry season leads to deep cracks in termite mounds [90], and termites construct or repair mounds to eliminate excessive water infiltration during heavy rain and reduce excessive water losses during the dry season [91]. Based on Cherian et al. [92], the electro-negativity of clay surfaces and their high adsorption capacity, which is due to the dissolution of clay minerals, may enhance the affinity of divalent cations, particularly calcium, in termite mounds. In general, enriched physicochemical properties, particularly clay, EC, avail. P, and, in some cases, K^+ and Na^+ in termite-mediated soils under open-grazing land, could be attributed to high termite activities depicted by the amount of soil translocated and mound erosion, where their intensity was higher in open-grazing land than in enclosures and cultivated land. The absence of significant differences observed in soil properties between the mound and the adjacent soil, as well as across different depths of the soil at the mound periphery, is likely due to erosion from the mounds.

4. Conclusions

We have explored that quantitative soil classification based on divisive clustering can identify soils within the same classes as the WRB classification system and can confirm the WRB soil classification. A key strength of the research lies in the fact that soil physicochemical properties are used to classify termite-mediated soils quantitatively. As a result, low pH, CEC, Ca^{2+} , and Mg^{2+} defined cambic horizons forming Cambisols, while high clay and CEC described argic horizons forming Luvisols. Calcisols are formed from a calcic horizon that is described by high pH, OC, Ca^{2+} , and Mg^{2+} . From this clustering, it can be concluded that numerical classification could be used for mapping termite-affected soils and evaluating existing soil variability. Agglomerative clustering reflects diagnostic horizons and pedogenic processes. The representative horizons of a given cluster were used for the first time to find patterns in termite-mediated soils, which could be used to predict soils in the same area that have not been studied. Termite bioturbation also plays an important role in soil property regulation, and rangeland use determines the impact on soil physicochemical properties. Soil turnover as a result of erosion from the mound results in similar soil properties between the mound and the adjacent soil. In addition, similar soil properties are found at different depths in the soil adjacent to the mound. Considering longevity and bioturbation, termite-induced pedogenesis may be more prominent on open-grazing land than under enclosure or cultivated land. Therefore, land use should be considered in determining the magnitude of termite-affected soils. Moreover, the results indicate that numerical classification is a promising complementary method to WRB soil classification. This study, however, demonstrated a limited aspect of numerical classification in describing termite-mediated soils, and therefore, future studies into other soil types are worthwhile.

Funding statement

This research was partially funded by the Ethiopian Ministry of Education through Ph.D. student subsidiary funds.

Data availability statement

Data will be made available on request.

CRediT authorship contribution statement

Abinet Bekele: Writing – original draft, Project administration, Methodology, Investigation, Formal analysis, Data curation, Conceptualization. **Sheleme Beyene:** Writing – review & editing, Validation, Supervision, Project administration. **Fantaw Yimer:** Writing – review & editing. **Alemayehu Kiflu:** Writing – review & editing.

Declaration of competing interest

The authors declare the following financial interests/personal relationships which may be considered as potential competing interests: Abinet Bekele reports financial support was provided by Ethiopian Ministry of Education. If there are other authors, they declare that they have no known competing financial interests or personal relationships that could have appeared to influence the work reported in this paper.

Acknowledgments

The authors gratefully acknowledge the unreserved support of the Soil and Plant Nutrition Laboratory, Hawassa University, Ethiopia. We would like to thank, Mr. Duguma Bekele Genale for his kind assistance during the fieldwork.

Appendix A. Supplementary data

Supplementary data to this article can be found online at <https://doi.org/10.1016/j.heliyon.2023.e23726>.

References

- [1] A. Bekele, S. Beyene, A. Kifu, F. Yimer, Genesis and classification of termite-mediated soils along toposequences in a semiarid area of southeast Ethiopia, *Appl. Environ. Soil Sci.* (2023), 7150907, <https://doi.org/10.1155/2023/7150907>.
- [2] S.K. Leclaire, M. Mdluli, S.M. Wisely, N. Stevens, Land-use diversity within an agricultural landscape promotes termite nutrient cycling services in a southern African savanna, *Glob. Ecol. Conserv.* 21 (2020), e00885, <https://doi.org/10.1016/j.gecco.2019.e00885>.
- [3] N. Subekti, R. Mar'ah, Estimating population size for *Macrotermes gilvus* hagen (blattoidea: termitidae) in Indonesia, *J. Phys. Conf. Ser.* 1321 (2019), 032050, <https://doi.org/10.1088/1742-6596/1321/3/032050>.
- [4] C. Chen, W. Liu, J. Wu, X. Jiang, Spatio-temporal variations of carbon and nitrogen in biogenic structures of two fungus-growing termites (*M. annandalei* and *O. yunnanensis*) in the Xishuangbanna region, *Soil Biol. Biochem.* 117 (2018) 125–134, <https://doi.org/10.1016/j.soilbio.2017.11.018>.
- [5] P. Jouquet, L. Caner, N. Bottinelli, E. Chaudhary, S. Cheik, J. Riotte, Where do South-Indian termite mound soils come from? *Appl. Soil Ecol.* 117 (118) (2017) 190–195, <https://doi.org/10.1016/j.apsoil.2017.05.010>.
- [6] J. Van Thuyne, I. Darini, A. Mainga, E.P. Verrecchia, Are fungus-growing termites super sediment-sorting insects of subtropical environments, *J. Arid Environ.* 193 (2021), 104566, <https://doi.org/10.1016/j.jaridenv.2021.104566>.
- [7] P. Jouquet, et al., The distribution of Silicon in soil is influenced by termite bioturbation in South Indian forest soils, *Geoderma* 372 (2020), 114362, <https://doi.org/10.1016/j.geoderma.2020.114362>.
- [8] P. Lavelle, et al., Soil invertebrates and ecosystem services, *Eur. J. Soil Biol.* 42 (2006) S3–S15, <https://doi.org/10.1016/j.ejsobi.2006.10.002>.
- [9] H.S. Badawy, Termite nests, rhizoliths and pedotypes of the Oligocene fluviomarine rock sequence in northern Egypt: proxies for Tethyan tropical palaeoclimates, *Palaeogeogr. Palaeoecol.* 492 (2018) 161–176, <https://doi.org/10.1016/j.palaeo.2017.12.021>.
- [10] J. Muvengwi, M. Mbiba, H.G.T. Ndagurwa, N. Kabvuratsiye, Pulsing hydrology and topography determine the structure and spatial distribution of *Cubitermes* mounds in a savanna ecosystem, *Catena* 145 (2016) 99–106, <https://doi.org/10.1016/j.catena.2016.05.009>.
- [11] J. Muvengwi, E.T.F. Witkowski, Cascading effects of termite mounds in African savannas, *New Zeal. J. Bot.* (2020), <https://doi.org/10.1080/0028825X.2020.1767162>.
- [12] C.J. Carey, J. Weverka, R. Digaudio, T. Gardali, E.L. Porzig, Exploring variability in rangeland soil organic carbon stocks across California (USA) using a voluntary monitoring network, *Geoderma* Reg 22 (2020), e00304, <https://doi.org/10.1016/j.geodrs.2020.e00304>.
- [13] T. Negasa, H. Ketema, A. Legesse, M. Sisay, H. Temesgen, Variation in soil properties under different land use types managed by smallholder farmers along the toposequence in southern Ethiopia, *Geoderma* 290 (2017) 40–50, <https://doi.org/10.1016/j.geoderma.2016.11.021>.
- [14] D. Kaiser, M. Lepage, S. Konaté, K.E. Linsenmair, Ecosystem services of termites (Blattoidea: termitidae) in the traditional soil restoration and cropping system Zaï in northern Burkina Faso (West Africa), *Agric. Ecosyst. Environ.* 236 (2017) 198–211, <https://doi.org/10.1016/j.agee.2016.11.023>.
- [15] N.C. Kanyih, H. Karuri, J.O. Nyasani, B. Mwangi, Land use effects on termite assemblages in Kenya, *Heliyon* 7 (2021), e08588, <https://doi.org/10.1016/j.heliyon.2021.e08588>.
- [16] C.M. Gosling, J.P.G.M. Crowsigt, N. Mpanza, H. Olff, Effects of erosion from mounds of different termite genera on distinct functional grassland types in an African savannah, *Ecosystems* 15 (2012) 128–139, <https://doi.org/10.1007/s10021-011-9497-8>.
- [17] S. Beyene, Topographic positions and land use impacted soil properties along Humbo Larena-Ofa Sere, *J. Soil Sci. Environ. Manag.* 8 (8) (2017) 135–147, <https://doi.org/10.5897/JSEM2017.0643>.
- [18] D. Dessalegn, S. Beyene, N. Ram, F. Walley, T.S. Gala, Effects of topography and land use on soil characteristics along the toposequence of Ele watershed in southern Ethiopia, *Catena* 115 (2014) 47–54, <https://doi.org/10.1016/j.catena.2013.11.007>.
- [19] *Soil Survey Staff, Keys to Soil Taxonomy*. United States Department of Agriculture, Natural Resources Conservation Service, 12th ed., twelfth ed., United States Department of Agriculture, Natural Resources Conservation Service, 2014.
- [20] IUSS Working Group WRB, World Reference Base for Soil Resources. *International Soil Classification System for Naming Soils and Creating Legends for Soil Maps*, fourth ed., International Union of Soil Sciences (IUSS), Vienna, Austria, 2022.
- [21] F.J. Young, R.D. Hammer, Defining geographic soil bodies by landscape position, soil taxonomy, and cluster analysis, *Soil Sci. Soc. Am. J.* 64 (2000) 989–998.
- [22] I. Esfandiarpour-Boroujenia, Z. Moslehb, M.H. Farpoor, Comparing soil taxonomy and WRB systems to classify soils with clay-enriched horizons (A case study: arid and semi-arid regions of Iran), *Desert* 23 (2) (2018) 315–325.
- [23] D. Balla, T.J. Novák, E. Kiss, T. Mester, G. Karancsi, M. Zichar, Classification and geovisualization process of soil data using a web-based spatial information system, *Open Agric* 5 (2020) 638–655, <https://doi.org/10.1515/opag-2020-0054>.
- [24] J.G. Bockheim, A.N. Gennadiyev, The role of soil-forming processes in the definition of taxa in soil taxonomy and the world soil reference base, *Geoderma* 95 (2000) 53–72.
- [25] E. Michéli, V. Láng, P.R. Owens, A. Mcbratney, J. Hempel, “Testing the pedometric evaluation of taxonomic units on soil taxonomy — a step in advancing towards a universal soil classification system.”, *Geoderma* (2015) <https://doi.org/10.1016/j.geoderma.2015.09.008>.
- [26] A. Deressa, M. Yli-halla, M. Mohamed, L. Wogi, Soil classification of humid Western Ethiopia: a transect study along a toposequence in Didessa watershed, *Catena* 163 (2018) 184–195, <https://doi.org/10.1016/j.catena.2017.12.020>.
- [27] D.E. Beaudette, P. Roudier, A.T. O'Geen, Algorithms for quantitative pedology: a toolkit for soil scientists, *Comput. Geosci.* 52 (2013) 258–268, <https://doi.org/10.1016/j.cageo.2012.10.020>.

- [28] F. Carré, M. Jacobson, Numerical classification of soil profile data using distance metrics, *Geoderma* 148 (2009) 336–345, <https://doi.org/10.1016/j.geoderma.2008.11.008>.
- [29] J.J. Maynard, S.W. Salley, D.E. Beaudette, J.E. Herrick, Numerical soil classification supports soil identification by citizen scientists using limited, simple soil observations, *Soil Sci. Soc. Am. J.* (September 2019) (2020) 1–18, <https://doi.org/10.1002/saj2.20119>.
- [30] V.A. Rozhkov, Formal apparatus of soil classification, *Eurasian Soil Sci.* 44 (12) (2011) 1289–1303, <https://doi.org/10.1134/S1064229311120106>.
- [31] P. Hughes, A.B. Mcbratney, J. Huang, B. Minasny, E. Micheli, J. Hempel, A nomenclature algorithm for a potentially global soil taxonomy, *Geoderma* 322 (2018) 56–70, <https://doi.org/10.1016/j.geoderma.2018.02.020>.
- [32] F. Shahbazi, J. Huang, A.B. Mcbratney, P. Hughes, Allocating soil profile descriptions to a novel comprehensive soil classification system, *Geoderma* 329 (2018) 54–60, <https://doi.org/10.1016/j.geoderma.2018.05.017>.
- [33] P.A. Hughes, A.B. Mcbratney, B. Minasny, S. Campbell, End members, end points and extragrades in numerical soil classification, *Geoderma* 226 (227) (2014) 365–375, <https://doi.org/10.1016/j.geoderma.2014.03.010>.
- [34] A. Eger, N. Koele, T. Caspari, M. Poggio, K. Kumar, O.R. Burge, Quantifying the importance of soil-forming factors using multivariate soil data at landscape scale, *J. Geophys. Res. Earth Surf.* 126 (2021), e2021JF006198, <https://doi.org/10.1029/2021JF006198>.
- [35] S.J. Park, T.P. Burt, Identification and characterization of pedogeomorphological processes on a hillslope, *Soil Sci. Soc. Am. J.* 66 (2002) 1897–1910.
- [36] I.O.A. Odeh, D.J. Chittleborough, A.B. Mcbratney, Elucidation of soil-landform interrelationships by canonical ordination analysis, *Geoderma* 49 (1991) 1–32.
- [37] D. Vasu, S.K. Singh, P. Tiwary, P. Chandran, S.K. Ray, V.P. Duraisami, Pedogenic processes and soil – landform relationships for identification of yield-limiting soil properties, *Soil Res.* (2016), <https://doi.org/10.1071/SR16111>.
- [38] M. Yemefack, D.G. Rossiter, R. Njomgang, Multi-scale characterization of soil variability within an agricultural landscape mosaic system in southern Cameroon, *Geoderma* 125 (2005) 117–143, <https://doi.org/10.1016/j.geoderma.2004.07.007>.
- [39] P. Hughes, A.B. Mcbratney, J. Huang, B. Minasny, E. Micheli, J. Hempel, Comparisons between USDA Soil Taxonomy and the Australian Soil Classification System I: data harmonization, calculation of taxonomic distance and inter-taxa variation, *Geoderma* 307 (2017) 198–209, <https://doi.org/10.1016/j.geoderma.2017.08.009>.
- [40] FAO, Lecture notes on the major soils of the world, in: *World Soil Resources Reports*, vol. 94, Food and Agriculture Organization of the United Nations, Rome, 2001, p. 334.
- [41] D. Patel, M.S. Rathore, M. Chandrashekaraiah, R.K. Singh, R.B. Sinha, A. Sahay, Infestation behaviour of termites on *Terminalia arjuna* and their management in the field, *J. Entomol. Zool. Stud.* 6 (6) (2018) 1226–1229.
- [42] T.S. Sarcinelli, C.E.G.R. Schaefer, E.I.F. Filho, R.G. Mafia, A.V. Neri, Soil modification by termites in a sandy-soil vegetation in the Brazilian Atlantic rain forest, *J. Trop. Ecol.* (2013), <https://doi.org/10.1017/S0266467413000497>.
- [43] D.F. De Freitas, J.C. Ker, L.A. da S. Filho, T.T.C. Pereira, O.F.F. de Souza, C.E.G.R. Schaefer, Pedogeomorphology and paleoenvironmental implications of large termite mounds at the Brazilian semi-arid landscape, *Geomorphology* 387 (2021), 107762, <https://doi.org/10.1016/j.geomorph.2021.107762>.
- [44] H.J. de Souza, J.H.C. Delabie, G.A. Sodré, Termite participation in the soil-forming processes of ‘murundus’ structures in the semi-arid region of Brazil, *Rev Bras Cienc Solo* 44 (2020), e0190133, <https://doi.org/10.36783/18069657rbc02190133>.
- [45] J.H. Görres, *Variability*, in: R. Lal (Ed.), *Encyclopedia of Soil Science*, third ed., CRC Press, 2017, pp. 2419–2427.
- [46] A. Salvucci, et al., Zoogenic soil horizons – termite ecosystem engineers in different agro-ecological regions of Mozambique, *Geoderma Reg* 32 (2023), e00618, <https://doi.org/10.1016/j.geodrs.2023.e00618>.
- [47] H.S. Pinheiro, L.H.C. dos Anjos, P.A. Xavier, C.S. Chagas, W. de C. Junior, Quantitative pedology to evaluate a soil profile collection from the Brazilian semi-arid region, *South African J. Plant Soil* (2018) 1–11, <https://doi.org/10.1080/02571862.2017.1419385>.
- [48] L. Tamene, Z. Adimassu, E. Aynekulu, T. Yaekob, Estimating landscape susceptibility to soil erosion using a GIS-based approach in Northern Ethiopia, *Int. Soil Water Conserv. Res.* 5 (2017) 221–230, <https://doi.org/10.1016/j.iswcr.2017.05.002>.
- [49] K. Vancampenhouta, et al., *Geoderma*, *Geoderma* 438 (2023), 116642, <https://doi.org/10.1016/j.geoderma.2023.116642>.
- [50] R.R. Weil, N.C. Brady, *The Nature and Properties of Soils*, fifteenth ed., Pearson Education Limited, England, 2017.
- [51] K.R. Olson, M.M. Al-kaisi, The importance of soil sampling depth for accurate account of soil organic carbon sequestration, storage, retention and loss, *Catena* 125 (2015) 33–37, <https://doi.org/10.1016/j.catena.2014.10.004>.
- [52] J. Bouma, et al., How can pedology and soil classification contribute towards sustainable development as a data source and information carrier, *Geoderma* 424 (2022), 115988, <https://doi.org/10.1016/j.geoderma.2022.115988>.
- [53] K. Feyisa, et al., Effects of enclosure management on carbon sequestration, soil properties and vegetation attributes in East African rangelands, *Catena* 159 (2017) 9–19, <https://doi.org/10.1016/j.catena.2017.08.002>.
- [54] N.G. Bikilaa, Z.K. Tessemab, E.G. Abule, Carbon sequestration potentials of semi-arid rangelands under traditional management practices in Borana, Southern Ethiopia, *Agric. Ecosyst. Environ.* 223 (2016) 108–114, <https://doi.org/10.1016/j.agee.2016.02.028>.
- [55] K. Ebabu, et al., Exploring the variability of soil properties as influenced by land use and management practices: a case study in the Upper Blue Nile basin, Ethiopia, *Soil Tillage Res.* 200 (2020), 104614, <https://doi.org/10.1016/j.still.2020.104614>.
- [56] X. Yao, N. Zhang, H. Zeng, W. Wang, Effects of soil depth and plant – soil interaction on microbial community in temperate grasslands of northern China, *Sci. Total Environ.* 630 (2018) 96–102, <https://doi.org/10.1016/j.scitotenv.2018.02.155>.
- [57] B.P. Akinde, A.O. Olakayode, D.J. Oyedele, F.O. Tijani, Selected physical and chemical properties of soil under different agricultural land-use types in Ile-Ife, Nigeria, *Heliyon* 6 (2020), e05090, <https://doi.org/10.1016/j.heliyon.2020.e05090>.
- [58] D.G. Debelo, Faunal survey of the termites of the genus *Macrotermes* (isoptera: termitidae) of Ethiopia, *J. Entomol. Nematol.* 10 (7) (2018) 50–64, <https://doi.org/10.5897/JEN2018.0216>.
- [59] B.E. Ó Dochaigh, *User Guide: Africa Groundwater Atlas Country Hydrogeology Maps, Version 1.0*, British Geological Survey Open Report, 2019. Or/19/035. 21pp.
- [60] FAO, Guidelines for field soil descriptions, in: Publishing Management Service Information Division, FAO (*Food And Agriculture Organization*), fourth ed., Fourth. Rome: Food and Agriculture Organization of the United Nations, Rome, 2006.
- [61] A. Tilahun, et al., Quantifying the masses of *Macrotermes subhyalinus* mounds and evaluating their use as a soil amendment, *Agric. Ecosyst. Environ.* 157 (2012) 54–59, <https://doi.org/10.1016/j.agee.2011.11.013>.
- [62] G.J. Bouyoucos, A recalibration of the hydrometer method for making mechanical analysis of soils, *Agron. J.* 43 (1951) 434–438.
- [63] D.W. Nelson, L.E. Sommers, Total carbon, organic carbon, and organic matter, in: A.L. Page, R.H. Miller, D.R. Keeney (Eds.), *Methods of Soil Analysis: Chemical and Microbiological Properties*, No 9 (Part 2) in the Series Agronomy, second ed., American Society of Agronomy, Inc. and Soil Science Society of America, Inc., Madison, Wisconsin, USA, 1982, pp. 539–577.
- [64] S.R. Olsen, C.V. Cole, F.S. Watanabe, L.A. Dean, Estimation of Available Phosphorus in Soils by Extraction with Sodium Bicarbonate, vol. 939, *USDA Circ.*, 1954, pp. 1–19.
- [65] H.D. Chapman, Cation-exchange capacity by ammonium saturation, in: C.A. Black, D.D. Evans, L.E. Ensminger, J.L. White, F.E. Clark, R.C. Dinauer (Eds.), *Methods of Soil Analysis, Agronomy Part II*, No. 9, American Society of Agronomy, Inc., Madison, Wisconsin, USA, 1965, pp. 891–901.
- [66] G.W. Thomas, Exchangeable cations, in: A.L. Page, R.H. Miller, D.R. Keeney (Eds.), *Methods of Soil Analysis: Chemical and Microbiological Properties*, No 9 (Part 2) in the Series Agronomy, second ed., American Society of Agronomy, Inc. and Soil Science Society of America, Inc., Madison, Wisconsin, USA, 1982, pp. 159–164.
- [67] FAO, “Standard operating procedure for soil calcium carbonate equivalent, 2020, in: *Titrimetric Method*. Food and Agriculture Organization, FAO) of the United Nations Rome, Rome, 2020, p. 16.
- [68] K.M. Yeater, M.B. Villamil, Multivariate methods for agricultural research, in: B. Glaz, K.M. Yeater (Eds.), *Applied Statistics in Agricultural, Biological, and Environmental Sciences*, American Society of Agronomy, Madison, Wisconsin, USA, 2018, pp. 371–400.
- [69] A. Kassambara, *Practical Guide to Principal Component Methods in R*, STHDA, 2017.

- [70] R Core Team, "R: A Language and Environment for Statistical Computing.", R Foundation for Statistical Computing, Vienna, Austria, 2021 [Online]. Available: <https://www.r-project.org>.
- [71] B. Labaz, E. Muszyfaga, J. Waroszewski, A. Bogacz, P. Jezierski, C. Kabala, Landscape-related transformation and differentiation of chernozems – catenary approach in the silesian lowland, SW Poland, *Catena* 161 (2018) 63–76, <https://doi.org/10.1016/j.catena.2017.10.003>.
- [72] E. Van Ranst, F. Mees, E. De Grave, L. Ye, J. Cornelis, B. Delvaux, Impact of andosolization on pedogenic Fe oxides in ferrallitic soils, *Geoderma* 347 (2019) 244–251, <https://doi.org/10.1016/j.geoderma.2019.04.013>.
- [73] B. Dinssa, E. Elias, Characterization and classification of soils of bako tibe district, west shewa, Ethiopia, *Heliyon* 7 (2021), e08279, <https://doi.org/10.1016/j.heliyon.2021.e08279>.
- [74] I.A. de Oliveira, J.M. Júnior, M.C.C. Campos, R.E. de Aquino, L. de Freitas, A.S. Ferraudo, Multivariate technique for determination of soil pedoenvironmental indicators in Southern Amazonas, *Acta Sci.* 39 (1) (2017) 99–108, <https://doi.org/10.4025/actasciagron.v39i1.30763>.
- [75] H.F. Teng, R.A.V. Rossel, R. Webster, A multivariate method for matching soil classification systems, with an Australian example, *Soil Res.* (2020), <https://doi.org/10.1071/SR19320>.
- [76] E. Bonifacio, G. Falsone, G. Simonov, T. Sokolova, I. Tolpeshta, Pedogenic processes and clay transformations in bisequal soils of the Southern Taiga zone, *Geoderma* 149 (1–2) (2009) 66–75, <https://doi.org/10.1016/j.geoderma.2008.11.022>.
- [77] J.J. Anyango, et al., The impact of conventional and organic farming on soil biodiversity conservation: a case study on termites in the long-term farming systems comparison trials in Kenya, *BMC Ecol.* 20 (13) (2020), <https://doi.org/10.1186/s12898-020-00282-x>.
- [78] S. Cheik, R.R. Shanbhag, A. Harit, N. Bottinelli, R. Sukumar, P. Jouquet, Linking termite feeding preferences and soil physical functioning in southern-Indian woodlands, *Insects* 10 (4) (2019), <https://doi.org/10.3390/insects10010004>.
- [79] C. Sanabria, F. Dubs, P. Lavelle, S.J. Fonte, S. Barot, Influence of regions, land uses and soil properties on termite and ant communities in agricultural landscapes of the Colombian Llanos, *Eur. J. Soil Biol. J.* 74 (2016) 81–92, <https://doi.org/10.1016/j.ejsobi.2016.03.008>.
- [80] D. Bera, S. Bera, N. Das Chatterjee, Termite Mound Soil Properties in West Bengal, India, vol. 22, *Geoderma Reg.* 2020, e00293, <https://doi.org/10.1016/j.geodrs.2020.e00293>.
- [81] E.H. Duran-Bautista, et al., Termites as indicators of soil ecosystem services in transformed amazon landscapes, *Ecol. Indic.* 117 (2020), 106550, <https://doi.org/10.1016/j.ecolind.2020.106550>.
- [82] S. Damene, L. Tamene, P.L.G. Vlek, Performance of enclosure in restoring soil fertility: a case of Gubalafto district in North Wello Zone, northern highlands of Ethiopia, *Catena* 101 (2013) 136–142, <https://doi.org/10.1016/j.catena.2012.10.010>.
- [83] P. Jouquet, M. Lepage, B. Velde, Termite soil preferences and particle selections: strategies related to ecological requirements, *Insectes Soc.* 49 (2002) 1–7.
- [84] K. Chisanga, E.R. Mbega, P.A. Ndademi, Prospects of using termite mound soil organic amendment for enhancing soil nutrition in southern africa, *Plants* 9 (649) (2020), <https://doi.org/10.3390/plants9050649>.
- [85] B.J. Enagbonma, O.O. Babalola, Potentials of termite mound soil bacteria in ecosystem engineering for sustainable agriculture, *Ann. Microbiol.* 69 (2019) 211–219, <https://doi.org/10.1007/s13213-019-1439-2>.
- [86] P. Sapountzis, J. De Verges, K. Rousk, M. Cilliers, B.J. Vorster, M. Poulsen, Potential for nitrogen fixation in the fungus-growing termite symbiosis, *Front. Microbiol.* 7 (2016) 1993, <https://doi.org/10.3389/fmicb.2016.01993>.
- [87] C.L. Seymour, et al., Do the large termite mounds of Macrotermes concentrate micronutrients in addition to macronutrients in nutrient-poor African savannas? *Soil Biol. Biochem.* 68 (2014) 95–105, <https://doi.org/10.1016/j.soilbio.2013.09.022>.
- [88] A.J. Mills, A. Milewski, M. V Fey, A. Groengroeft, A. Petersen, Fungus culturing, nutrient mining and geophagy: a geochemical investigation of Macrotermes and Trinervitermes mounds in southern Africa, *J. Zool.* 278 (2009) 24–35, <https://doi.org/10.1111/j.1469-7998.2008.00544.x>.
- [89] Y. Cheng, et al., Effects of soil erosion and land use on spatial distribution of soil total phosphorus in a small watershed on the Loess Plateau, China, *Soil Tillage Res.* 184 (2018) 142–152, <https://doi.org/10.1016/j.still.2018.07.011>.
- [90] P. Jouquet, N. Guilleux, L. Caner, S. Chintakunta, M. Ameline, R.R. Shanbhag, Influence of soil pedological properties on termite mound stability, *Geoderma* 262 (2016) 45–51, <https://doi.org/10.1016/j.geoderma.2015.08.020>.
- [91] C. Chen, et al., Hydrological characteristics and functions of termite mounds in areas with clear dry and rainy seasons, *Agric. Ecosyst. Environ.* 277 (2019) 25–35, <https://doi.org/10.1016/j.agee.2019.03.001>.
- [92] C. Cherian, N.J. Kollannur, S. Bandipally, D.N. Arnepalli, Calcium adsorption on clays: effects of mineralogy, pore fluid chemistry and temperature, *Appl. Clay Sci.* (2018), <https://doi.org/10.1016/j.clay.2018.02.034>.